Supplementary figures

Figure S1.

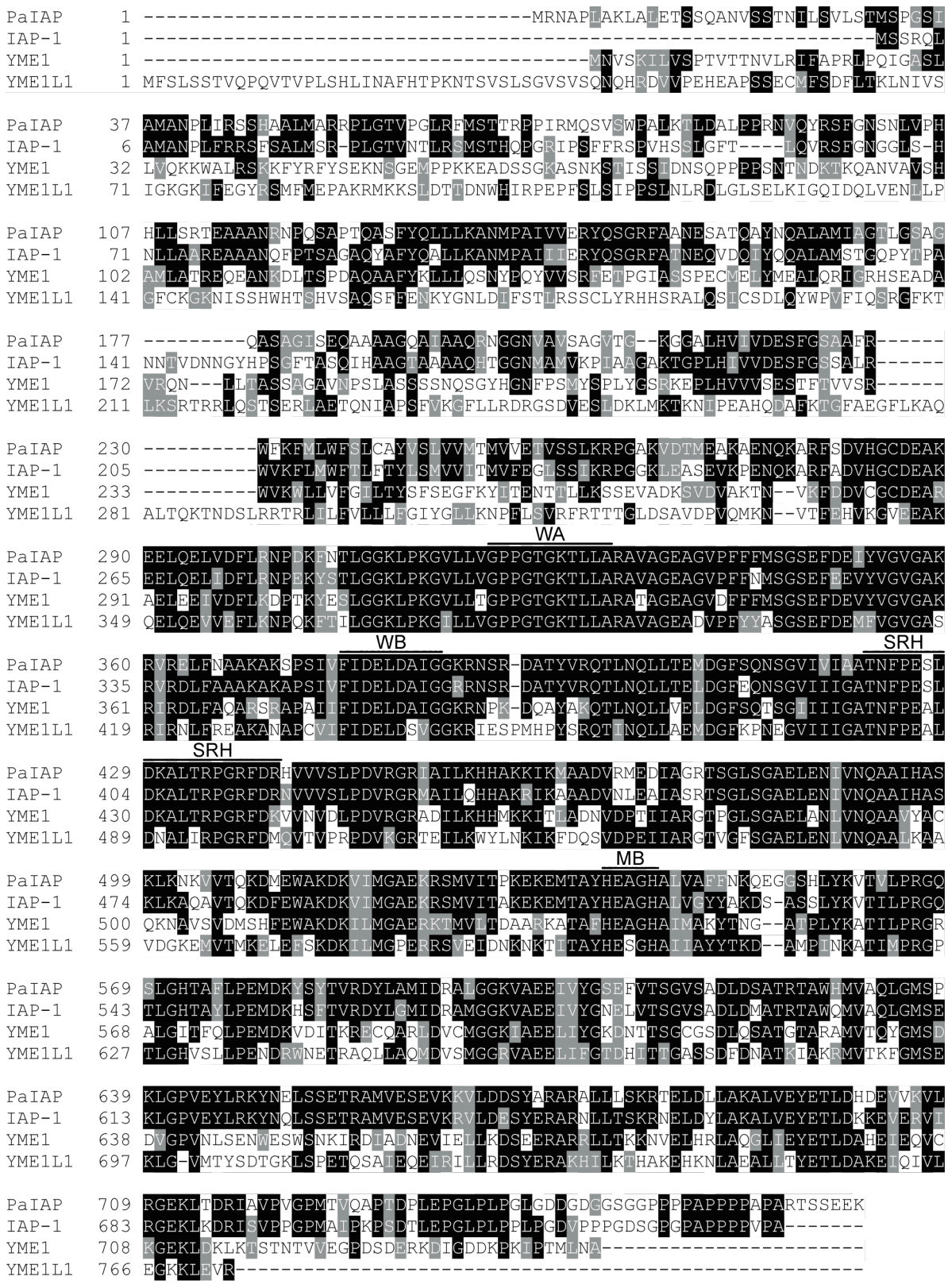

Figure S1. Sequence alignment of i-AAA protease subunits of *P. anserina*, *N. crassa*, *S. cerevisiae* and *H. sapiens*. The sequences of PaIAP of *P. anserina*, IAP-1 of *N. crassa*, YME1 of *S. cerevisiae* and YME1L1 of *H. sapiens* were aligned using the program ClustalW (version 1.83). Identical amino acid residues in all four sequences are shown white on black. Amino acid residues that are conserved in the sequences are shaded in gray. The Walker A (WA) and Walker B (WB) motifs, the second region of homology (SRH), which are characteristic of the AAA family of ATPases, and the consensus metal binding motifs (ME), representing the putative catalytic centers, are indicated.

Figure S2.

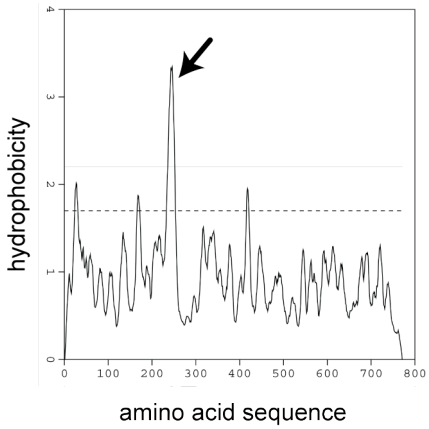

Figure S2. Hydrophobicity profile of PalAP. The presence of a transmembrane region in the amino acid sequence of PalAP was analyzed using the DAS software (www.sbc.su.se/~miklos/DAS). The hydrophobic region that presents the predicted transmembrane domain is indicated by an arrow.

Figure S3.

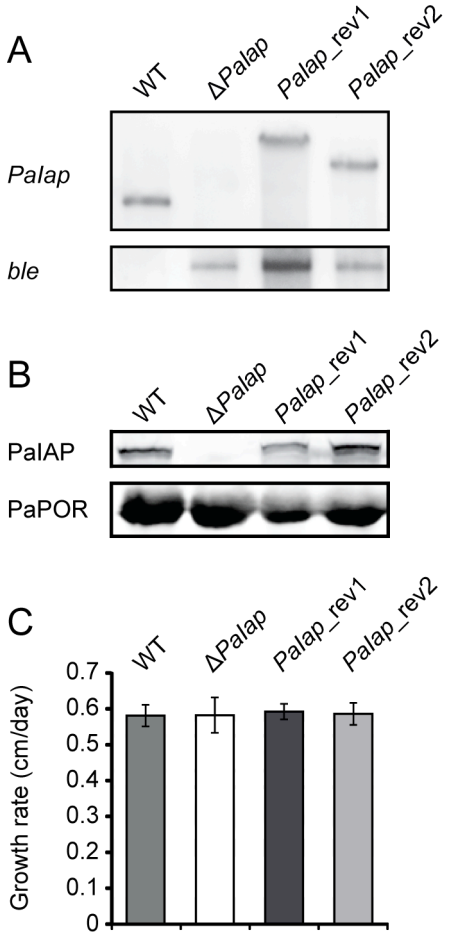

Figure S3. Reintroduction of *Palap* into Δ*Palap* leads to a wild-type like phenotype. (A) Southern blot analyses of *Bgl*II digested DNA from the WT, Δ*Palap* and *Palap* deletion strains in which the ORF of *Palap* under the control of its own promoter and terminator has been reintroduced (*Palap*_rev). A *Palap* specific probe reveals that *Palap*_rev1 and 2 carry a single copy of the *Palap* wild-type gene. (B) Western blot analyses of mitochondrial proteins from the WT, Δ*Palap* and *Palap*_rev1 and 2. The PaIAP specific antibody detects PaIAP in mitochondria of the WT as well as in mitochondria from *Palap*_rev1 and 2 (upper panel). PaPOR was used as loading control (lower panel). (C) Growth rates of the WT (n = 71), Δ*Palap* (n = 73), *Palap*_rev1 (n = 59) and *Palap*_rev2 (n = 40).

Figure S4.

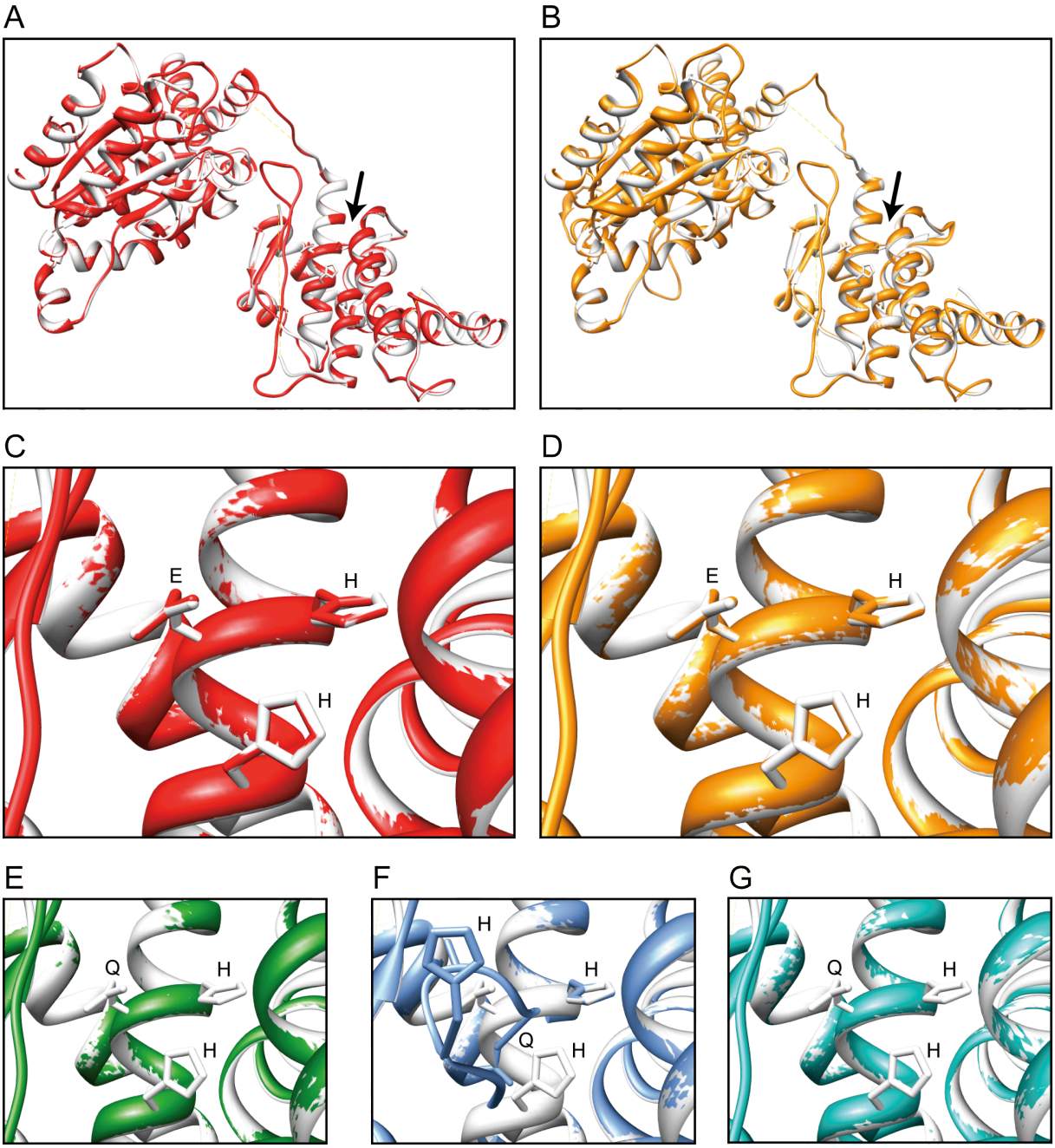

Figure S4. Models of the protein structures of PalAP and YME1 compared to their homologue FTSH from *Thermotoga maritima*. Ribbon view of FTSH from the bacterium *T. maritima* shown in white,[59] PalAP in red (A) and YME1 in orange (B). To estimate the effect of the mutation in the metal binding motif HEXXH on the structure of the i-AAA protease, we generated homology models for the structurally related proteins PalAP, YME1 and FTSH with SWISS-MODEL using the crystal structure of a soluble FTSH construct.[60] In the model, replacement of glutamic acid (E) to glutamine (Q) does not seem to change the structure of the helix in PalAP (red in (C) and green in (E)) and in YME1 (orange in (D) and turquoise in (G)). In contrast, the addition of glycine (G) in the metal binding motif of PalAP creating the

amino acid sequence HQGAGH possibly alters the structure of the helix (blue in (F)). The molecular graphics were produced using UCSF Chimera.[61]

Figure S5.

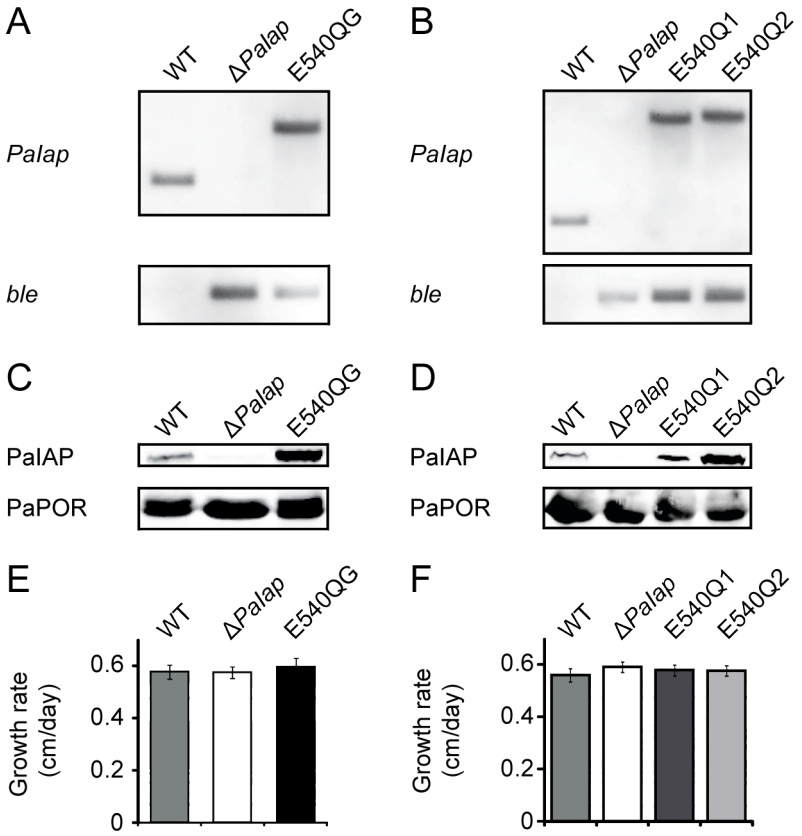

Figure S5. Manipulation of the proteolytic activity of PalAP. (A) and (B) Southern blot analyses of DNA from the WT, Δ*Palap* and *Palap* deletion strains in which the ORF of *Palap* carrying a mutation in the metal binding motif at amino acid position 540 (*Palap*_E540Q1 and 2) followed by glycine has been reintroduced (*Palap*_E540QG, *Palap*_E540Q1 and 2). A *Palap* specific probe shows the presence of one copy of the modified *Palap* gene in *Palap*_E540QG (E540QG), *Palap*_E540Q1 (E540Q1) and *Palap*_E540Q2 (E540Q2). (C) and (D) Western blot analyses of mitochondrial proteins from the WT, Δ*Palap*, *Palap*_E540QG (E540QG), *Palap*_E540Q1 (E540Q1) and from *Palap*_E540Q2 (E540Q2). PalAP can be detected in mitochondria of the WT as well as in samples from *Palap*_E540Q and *Palap*_E540QG (upper panel). PaPOR was used as loading control (lower panel). (E) Growth rates of the WT (n = 21), Δ*Palap* (n = 34) and *Palap*_E540QG (E540QG; n = 30). (F) Growth rates of the WT (n = 24), Δ*Palap* (n = 24), *Palap*_E540Q1 (E540Q1; n = 35) and *Palap*_E540Q2 (E540Q2; n = 27).

Reference list

59. Bieniossek C, Schalch T, Bumann M, Meister M, Meier R, Baumann U. The molecular architecture of the metalloprotease FtsH. Proc Natl Acad Sci USA 2006; 103: 3066-3071

60. Schwede T, Kopp J, Guex N, Peitsch MC. SWISS-MODEL: An automated protein homology-modeling server. Nucleic Acids Res 2003; 31: 3381-3385.

61. Pettersen EF, Goddard TD, Huang CC, Couch GS, Greenblatt DM, Meng EC, et al. UCSF Chimera--a visualization system for exploratory research and analysis. J Comput Chem 2004; 25: 1605-1612.